DC-Compliant Macromodels Based on the Method of Characteristics for Frequency-Dependent Transmission Lines

Stefano Grivet-Talocia, Flavio Canavero
Dipartimento di Elettronica, Politecnico di Torino
Corso Duca degli Abruzzi 24, 10129, Torino, Italy
stefano.grivet@polito.it

Abstract

This paper investigates a possible source of inaccuracy for transmission line macromodels based on the Method of Characteristics (MoC). We show that, for the general class of lines with a vanishing DC conductance, the standard procedure of delay extraction followed by a rational function approximation of characteristic admittance and delayless propagation operators may lead to a wrong DC behavior of the macromodel. This degeneracy may be resolved by a suitable perturbation on the DC conductance. We show that this perturbation can be designed in order to ensure arbitrary accuracy of the DC response of the macromodel, without affecting the accuracy and efficiency of the MoC formulation.

Introduction

Modeling and simulation of transmission line structures remains a very challenging task despite the extensive research work that has been dedicated to the subject over many years. The ultimate goal is a SPICE-compatible model of the transmission line, allowing for transient simulations of structures that are natively characterized via frequency-dependent parameters. Many different techniques have been proposed to handle this problem. We can cite standard lumped circuit segmentation [1], Matrix Rational Approximations (MRA) [7], and delay-extraction based techniques. Among the latter, we can distinguish the methods based on total delay extraction, usually denoted as Method of Characteristics (MoC) approaches [3-6] since the original lossless formulation by Branin [2], and the more recent methods based on Lie product decomposition [8]. Depending on the specific class of line under consideration, a specific method may be preferred. For instance, short lines with a negligible propagation delay may be efficiently described by segmentation or MRA approaches. On the other hand, these techniques become inefficient when the delay is comparable to or larger than the rise time of the signal waveforms. For these structures it is widely recognized that approaches based on the delay extraction are more efficient and should be preferred.

The focus of this paper is on MoC-based macromodels of frequency-dependent multi-conductor transmission lines. We consider the general class of lines with a per-unit-length conductance that is vanishing at zero frequency (DC). Most commonly-used models of lines on chip, chip carrier, board, and cables fall into this class. We show that the standard procedure for the MoC-based macromodel generation, i.e., the independent computation of rational approximations for both characteristic admittance and delayless propagation operators, does not allow the control of the macromodel accuracy under constant (DC) excitation. Clearly, this lack of accuracy poses serious limits to extensive use of the macromodel for system-level simulations using SPICE-like solvers. We show that this ill-posedness is due to a degeneracy of the macromodel topology at DC, which becomes not consistent with the DC transmission-line stamp.

The DC degeneracy does not occur when the DC per-unit-length conductance matrix is nonvanishing. This suggests a possible approach to overcome this difficulty, namely the introduction of a perturbation term in the macromodel corresponding to a small amount of shunt losses and consisting of a small DC per-unit-length conductance. A systematic derivation shows that the proposed stamp of the macromodel becomes fully DC compliant when this perturbation term is inserted. In addition, a sensitivity analysis allows to relate the deviation induced in the macromodel DC solution to the original perturbation term. Both analytical and numerical results show that the error on the computed DC solution can be made arbitrarily small by selecting an appropriate DC conductance value. Explicit rules for the determination of the perturbation DC conductance are provided for both single and multiconductor lines, under any given termination condition. In summary, the main contribution of this paper is a rigorously-derived practical rule enabling systematic use of MoC-based macromodels for any class of transmission line structures.

We set the notations in Section 1, and we state the main problem in Sections 2 and 3 for different classes of transmission lines. The proposed perturbation approach is detailed in Section 4. Finally, numerical results and validations are reported in Section 5. We remark that other important related issues like causality in the line specification and passivity of the MoC macromodel will not be considered in this work.

Background and notations

We consider a lossy multiconductor transmission line governed by the telegraphers equations, here stated in the Laplace domain

$$\frac{d\mathbf{V}(z,s)}{dz} = -\mathbf{Z}(s)\mathbf{I}(s)$$

$$\frac{d\mathbf{I}(z,s)}{dz} = -\mathbf{Y}(s)\mathbf{V}(s) \qquad (1)$$

where z represents the longitudinal coordinate along which signals propagate. The length of the line is L, and the number of signal conductors is N. Unless otherwise specified, all vectors and matrices in this paper have size N. The transmission line per-unit-length matrices $\mathbf{Y}(s)$ and $\mathbf{Z}(s)$ are defined as

$$\mathbf{Y}(s) = \mathbf{G}(s) + s\mathbf{C}(s), \quad \mathbf{Z}(s) = \mathbf{R}(s) + s\mathbf{L}(s) \quad (2)$$

with $\mathbf{G}(s), \mathbf{C}(s), \mathbf{R}(s), \mathbf{L}(s)$ denoting the per-unit-length conductance, capacitance, resistance, and inductance matrices, respectively. These matrices are usually known at fixed frequency points by means of transverse 2D electromagnetic simulations.

The MoC approach treats the transmission line segment as a multiport, with terminal voltages and currents denoted as $\mathbf{V}_1(s)$, $\mathbf{I}_1(s)$ and $\mathbf{V}_2(s)$, $\mathbf{I}_2(s)$, see Figure 1. In the MoC model, the solution of the Telegrapher's transmission line equations can be reduced to

$$\mathbf{B}_1(s) = \mathbf{H}(s)\mathbf{A}_2(s), \quad \mathbf{B}_2(s) = \mathbf{H}(s)\mathbf{A}_1(s) \quad (3)$$

where

$$\mathbf{A}_i(s) = \mathbf{Y}_C(s)\mathbf{V}_i(s) + \mathbf{I}_i(s)$$
$$\mathbf{B}_i(s) = \mathbf{Y}_C(s)\mathbf{V}_i(s) - \mathbf{I}_i(s) \qquad (4)$$

and with

$$\mathbf{\Gamma}^2(s) = \mathbf{Y}(s)\mathbf{Z}(s),$$
$$\mathbf{Y}_C(s) = \mathbf{\Gamma}^{-1}(s)\mathbf{Y}(s), \qquad (5)$$
$$\mathbf{H}(s) = \exp\{-L\mathbf{\Gamma}(s)\}$$

being the squared propagation matrix, the characteristic admittance matrix, and the propagation operator, respectively.
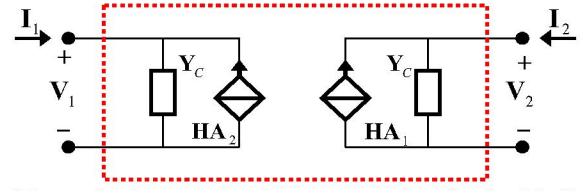

Figure 1: abstract circuit representation for the MoC line formulation.

The above expressions represent a set of implicit constitutive relations of a $2N$-port circuit element, which is represented in an abstract form in Figure 1. Simple algebraic manipulations can be used to obtain any standard explicit form like, e.g., admittance, scattering or transmission (chain) representations. We adopt the latter for the main derivations, noting that the same results would be obtained with the other representations. The chain matrix representation of the transmission line reads

$$\begin{pmatrix} \mathbf{V}_1(s) \\ \mathbf{I}_1(s) \end{pmatrix} = \begin{pmatrix} \mathbf{T}_{11}(s) & \mathbf{T}_{12}(s) \\ \mathbf{T}_{21}(s) & \mathbf{T}_{22}(s) \end{pmatrix} \begin{pmatrix} \mathbf{V}_2(s) \\ -\mathbf{I}_2(s) \end{pmatrix} \quad (6)$$

where

$$\mathbf{T}_{11}(s) = \tfrac{1}{2}\mathbf{Y}_C^{-1}(s)\left(\mathbf{H}^{-1}(s) + \mathbf{H}(s)\right)\mathbf{Y}_C(s),$$

$$\mathbf{T}_{12}(s) = \tfrac{1}{2}\mathbf{Y}_C^{-1}(s)\left(\mathbf{H}^{-1}(s) - \mathbf{H}(s)\right),$$

$$\mathbf{T}_{21}(s) = \tfrac{1}{2}\left(\mathbf{H}^{-1}(s) - \mathbf{H}(s)\right)\mathbf{Y}_C(s),$$

$$\mathbf{T}_{22}(s) = \tfrac{1}{2}\left(\mathbf{H}^{-1}(s) + \mathbf{H}(s)\right).$$

$$(7)$$

The key feature of MoC formulation is the extraction of the line propagation delay. This operation can be performed in different ways [6]. Here we consider the asymptotic modal delays collected in diagonal matrix $\mathbf{T}$,

$$\mathbf{T} = L\sqrt{\mathbf{\Lambda}} \qquad (8)$$

with $\mathbf{\Lambda}$ diagonal, obtained from the following eigendecomposition

$$\mathbf{C}(\infty)\mathbf{L}(\infty) = \mathbf{M}\mathbf{\Lambda}\mathbf{M}^{-1} \qquad (9)$$

A delayless propagation operator is obtained as

$$\mathbf{P}(s) = \exp\{s\mathbf{T}\}\mathbf{M}^{-1}\mathbf{H}(s)\mathbf{M} \qquad (10)$$

This operator acts on asymptotic modal waves and represents the dispersion and the losses occurring during propagation between the two line terminals. It is well known that the entries of $\mathbf{Y}_C(s)$ and $\mathbf{P}(s)$ are very smooth, thus the rational approximations

$$Y_C(s) \simeq \hat{Y}_C(s) = Y_\infty + \sum_n \frac{R_n^Y}{s - p_n}$$

$$P(s) \simeq \hat{P}(s) = P_\infty + \sum_n \frac{R_n^P}{s - q_n} \qquad (11)$$

can be computed quite easily with high accuracy [6] using standard least squares algorithms. We remark that throughout this paper, any macromodel (approximated) variable will be denoted by a hat sign to distinguish it from its exact counterpart. The above delay extraction procedure is indeed the main advantage of the MoC formulation, since the rapid phase variations of the propagation matrix $H(s)$ would make its direct rational approximation difficult and inefficient. A delayed rational approximation of the propagation operator is thus obtained as

$$H(s) \simeq \hat{H}(s) = M \exp\{-sT\}\hat{P}(s)M^{-1} \qquad (12)$$

The complete macromodel equations result identical to Eqs.(3)-(4), with the only difference being the substitution of exact admittance and propagation operators $Y_C(s)$ and $H(s)$ with their rational and delayed-rational approximations $\hat{Y}_C(s)$ and $\hat{H}(s)$, respectively. This MoC macromodel is well suited to SPICE-like realizations using time-delayed sources. Moreover, macromodel implementations using recursive convolutions are particularly fast and are widely recognized as the most efficient line solution methods for electrically long transmission line segments. We conclude this section by reporting the chain matrix representation for the MoC macromodel,

$$\hat{T}_{11}(s) = \tfrac{1}{2}\hat{Y}_C^{-1}(s)\left(\hat{H}^{-1}(s) + \hat{H}(s)\right)\hat{Y}_C(s),$$

$$\hat{T}_{12}(s) = \tfrac{1}{2}\hat{Y}_C^{-1}(s)\left(\hat{H}^{-1}(s) - \hat{H}(s)\right),$$

$$\hat{T}_{21}(s) = \tfrac{1}{2}\left(\hat{H}^{-1}(s) - \hat{H}(s)\right)\hat{Y}_C(s), \qquad (13)$$

$$\hat{T}_{22}(s) = \tfrac{1}{2}\left(\hat{H}^{-1}(s) + \hat{H}(s)\right)$$

DC compliance of MoC macromodels: lines with non-vanishing DC conductance

Let us first consider the general class of transmission lines having finite and non-vanishing (strictly positive-definite) per unit length resistance and conductance at zero frequency (DC), i.e.,

$$\lim_{s \to 0} Z(s) = R_0 > 0, \quad \lim_{s \to 0} Y(s) = G_0 > 0 \qquad (14)$$

The corresponding DC limits for all MoC-related variables are

$$\lim_{s \to 0} \Gamma(s) = \Gamma_0 = \sqrt{G_0 R_0},$$

$$\lim_{s \to 0} Y_C(s) = Y_{C0} = \left(\sqrt{G_0 R_0}\right)^{-1} G_0, \qquad (15)$$

and the DC limit for the exact chain matrix reads

$$T_0 = \begin{pmatrix} Y_{C0}^{-1} \text{ch}(\Gamma_0 L) Y_{C0} & Y_{C0}^{-1} \text{sh}(\Gamma_0 L) \\ \text{sh}(\Gamma_0 L) Y_{C0} & \text{ch}(\Gamma_0 L) \end{pmatrix}, \qquad (16)$$

where none of the matrix blocks is singular. A consistent DC behavior of the MoC macromodel is obtained if these DC limits are preserved. This can be easily accomplished if the rational approximations in Eq.(11) are computed by imposing the additional linear constraints

$$Y_\infty - \sum_n \frac{R_n^Y}{p_n} = Y_{C0},$$

$$P_\infty - \sum_n \frac{R_n^P}{q_n} = M^{-1} \exp\{-\Gamma_0 L\}M, \qquad (17)$$

as suggested in [6]. This procedure will make sure that the DC behavior of the macromodel will be automatically correct, i.e.,

$$\lim_{s \to 0} \hat{T}(s) = T_0 \qquad (18)$$

DC compliance of MoC macromodels: lines with vanishing DC conductance

Let us focus now on the particular case of lines having a vanishing per-unit-length DC conductance

$$\lim_{s \to 0} Y(s) = 0. \qquad (19)$$

A straightforward derivation leads to the DC limit of the exact chain matrix as

$$T_0 = \begin{pmatrix} 1 & R_0 L \\ 0 & 1 \end{pmatrix} \qquad (20)$$

which corresponds to the equivalent circuit depicted in Figure 2. The DC limits for propagation constant and characteristic admittance are both vanishing

$$\lim_{s \to 0} \Gamma(s) = 0$$

$$\lim_{s \to 0} Y_C(s) = 0 \qquad (21)$$

The explicit enforcement of the DC constraints in Eq.(17) leads in this case to an ill-defined macromodel, as depicted in Figure 3. In fact, a direct substitution of the above DC limits in the MoC formulation of Eqs.(3)-(4), leads to

$$I_1 + I_2 = 0 \qquad (22)$$

as the only constitutive relation of the macromodel at DC. It can be seen that this degeneracy is due to an inconsistent representation of the $\mathbf{T}_{12}$ block of the chain matrix.
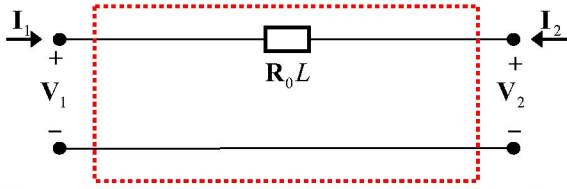

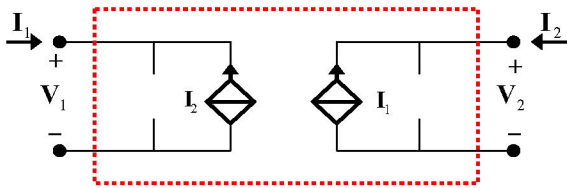Figure 2: equivalent DC circuit of a transmission line with vanishing DC conductance.

Figure 3: degeneracy of the MoC macromodel for a transmission line with vanishing DC conductance.

Previous implementations of the MoC macromodels such as TOPLine [6] handle this problem via an ad hoc procedure, by explicitly providing the SPICE kernel by a transmission line stamp which depends on the type of analysis. The DC stamp is provided by Eq.(20), where the transient analysis stamp is based on the standard MoC formulation. Unfortunately, this procedure is only possible when direct access to the SPICE kernel or to the MNA matrices is granted. In this work, we provide an alternative solution to this DC degeneracy, which does not require particular ad hoc implementations.

Accuracy-controlled DC regularization

We have already shown in Section 2 that the MoC formulation is automatically DC compliant when the DC conductance is non-vanishing. We exploit this fact to design a regularization procedure for the DC degeneracy also in the case of vanishing DC conductance.

The basic assumption that we make is a smooth dependence of the transmission line responses under small perturbations in the DC conductance. The formal proof of this fact is omitted here because of lack of space. This assumption allows for a series expansion of the transmission line chain matrix elements in Eq.(16) around $\mathbf{G}_0 \sim \mathbf{0}$. A straightforward derivation leads to

$$\mathbf{T}_0 \simeq \begin{pmatrix} 1 + \frac{1}{2}\Delta & \mathbf{R}_0 L\left(1 + \frac{1}{6}\Delta\right) \\ \mathbf{G}_0 L\left(1 + \frac{1}{6}\Delta\right) & 1 + \frac{1}{2}\Delta \end{pmatrix} \quad (23)$$

where $\Delta = \mathbf{G}_0 \mathbf{R}_0 L^2$. This expression leads to two conclusions.

1. If we perturb the per-unit-length admittance by adding a constant matrix term $\mathbf{G}_0$, the most important perturbation in the chain matrix is on the element $\mathbf{T}_{21} \simeq \mathbf{G}_0 L$. This results in a non-perfect consistency with the exact chain matrix of Eq.(20), but the deviation can be made as small as desired by choosing a small value for $\mathbf{G}_0$;

2. The leading error term in the expansion is $O(\Delta)$, which is proportional to the product of total DC resistance and conductance. Again, this term can be made as small as desired by choosing a small value for $\mathbf{G}_0$.

Based on the above conclusions, we suggest the following procedure for modeling transmission lines having vanishing DC conductance.

1. Modify the per-unit-length admittance by adding a small constant term. For simplicity, this term is assumed diagonal with identical elements G_0 on the main diagonal

$$\mathbf{Y}(s) \leftarrow \mathbf{Y}(s) + G_0 \mathbf{1} \quad (24)$$

2. Perform the macromodel generation as described in Section 2 for lines with a non-vanishing conductance.

As a result, the macromodel will be automatically DC compliant. The overall accuracy of the macromodel is kept under control by choosing an appropriate value for the scalar perturbation term G_0. This is detailed next.

The main practical metric to be considered for controlling the accuracy of the macromodel is the induced perturbation on the actual DC solution under a given termination scheme. To this end, we consider arbitrary linear Thevenin terminations

$$\mathbf{V}_1 = \mathbf{V}_S - \mathbf{Z}_S \mathbf{I}_1, \quad \mathbf{V}_2 = -\mathbf{Z}_L \mathbf{I}_2. \quad (25)$$

The nominal ($G_0 = 0$) DC solution for the far end voltage is

$$\mathbf{V}_2^{nom} = \mathbf{Z}_L \mathbf{Z}_{tot}^{-1} \mathbf{V}_S \quad (26)$$

where $\mathbf{Z}_{tot} = \mathbf{Z}_S + \mathbf{Z}_L + \mathbf{R}_0 L$ is the total series impedance seen by the voltage source. Denoting now

$$\delta\mathbf{Z} = \mathbf{Z}_S(G_0L)\mathbf{Z}_L \qquad (27)$$

we obtain, after a straightforward derivation, the induced perturbation on the nominal DC point as

$$\mathbf{V}_2 \simeq \mathbf{V}_2^{nom} - \mathbf{Z}_L\mathbf{Z}_{tot}^{-1}\,\delta\mathbf{Z}\,\mathbf{Z}_{tot}^{-1}\mathbf{V}_S \qquad (28)$$

The error on the DC point is therefore linearly related to the scalar perturbation term G_0. This implies that, for any given termination scheme, a suitable value for G_0 can be determined a priori in order to insure a given accuracy in the DC point.

In order to make the above considerations more explicit, we analyze the scalar transmission line case in detail, noting that the main conclusions will hold for the general multiconductor case. The relative error on the DC point for the scalar case reads

$$\varepsilon = \frac{Z_S(G_0L)Z_L}{Z_S + Z_L + R_0L + Z_S(G_0L)Z_L} \qquad (29)$$

From this expression, it is clear that the most critical case occurs in case of high-impedance loads. If, for instance we let the far end of the line open or capacitively loaded ($|Z_L| \to \infty$ at DC), we get

$$\varepsilon = \frac{Z_S(G_0L)}{1 + Z_S(G_0L)}. \qquad (30)$$

A practical rule is therefore to select a value for G_0 such that

$$(G_0L)Z \ll 1, \quad \forall Z \in \{Z_S, Z_L, R_0L\} \qquad (31)$$

Numerical examples

As an illustrative example, we consider a scalar transmission line with constant per-unit-length parameters $\mathbf{R} = 1\,\Omega/cm$, $\mathbf{L} = 4\,nH/cm$, $\mathbf{C} = 1\,pF/cm$, and $\mathbf{G} = 0$. The line length is varied from 1 cm up to 100 cm. The sensitivity of the DC solution to the perturbation DC conductance G_0 is investigated by sweeping its value from $10^{-9}\,mS/cm$ up to $10^{-3}\,mS/cm$, under varying termination conditions. For each individual case, a 10-poles rational approximation for characteristic admittance and delayless propagation operator is computed as in [6], the macromodel is implemented in SPICE as an external subcircuit, and the DC operating point is computed using PSPICE.

Figures 4 and 5 depict the relative error on the DC solution for both termination voltages using standard $50\,\Omega$ resistive terminations and for a line length of 1 cm and 100 cm, respectively. The linear

dependence of this relative error on the perturbation G_0 is evident from the plots. Note that the maximum relative accuracy (about 10^{-7}) of the adopted SPICE solver limits the dynamic range in which the linear dependence can be observed on the results.
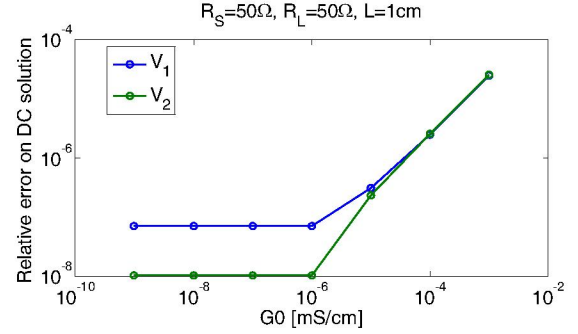
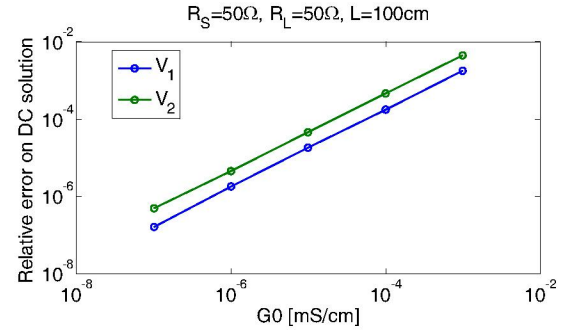Figure 4: sensitivity of DC solution under resistive terminations, L=1cm

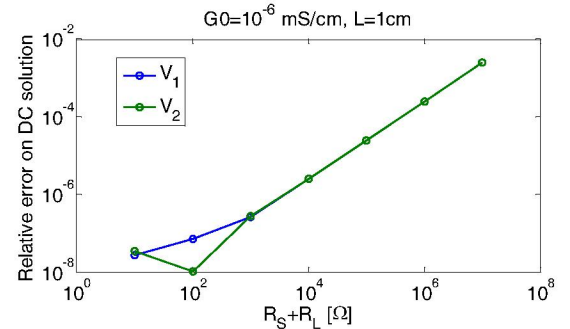Figure 5: sensitivity of DC solution under resistive terminations, L=100 cm

Figure 6: sensitivity of DC solution versus total load impedance, L=1cm

Figure 6 illustrates the dependence of the DC solution on the termination impedance for a fixed value $G_0 = 10^{-6}\,mS/cm$ and for a 1 cm line. This plot shows that the worst case occurs when the total termination impedance is largest. Therefore, the design of G_0 should be performed by considering the largest possible termination impedance for the particular application.

Figure 7 illustrates a worst-case scenario, corresponding to a capacitive load. For this case, also the absolute error on the input DC current (which should be vanishing) is plotted with the relative error on the DC termination voltages. This current returns through the shunt losses of the macromodel represented by the inserted DC conductance. Also in this limit case the value of G_0 can be determined based on the desired accuracy of the DC solution.
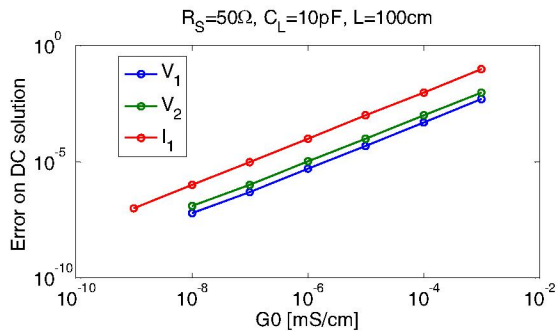

Figure 7: Relative (V) and absolute (I) error on DC solution under capacitive termination, L=100cm

Conclusions

We have presented a simple and effective procedure for handling a degeneracy affecting macromodels of transmission lines having vanishing DC conductance. This degeneracy occurs when the structure of the macromodel is based on the so-called Method of Characteristics. The proposed scheme involves a perturbation of the DC conductance by a small value, which can be designed in order to insure arbitrarily small errors in the macromodel responses.

References

1. C.R.Paul, Analysis of Multiconductor Transmission Lines, Wiley & Sons, (New York, 1994).
2. F.H.Branin, ``Transient Analysis of Lossless Transmission Lines", *Proc. IEEE*, Vol.55, 1967, pp.2012-2013.
3. S.Lin, E.S.Kuh, ``Transient simulation of lossy interconnects based on recursive convolution formulation", *IEEE Transactions on Circuits and Systems-I*, Vol.39, 1992, pp.879-892.
4. A.J.Gruodis, C.S.Chang, ``Coupled lossy transmission line characterization and simulation", *IBM Journal of Research and Development*, Vol.25, 1981, pp.25-41.
5. T.V.Ngyuen, ``Transient analysis of lossy transmission lines using rational function approximations", in *Digest of Electr. Perf. Electronic Packaging*, Vol.2, 20-22 October, 1993, pp.172-174.
6. S.Grivet-Talocia, H.-M.Huang, A.E. Ruehli, F.Canavero, and I.M. Elfadel, ``Transient analysis of lossy transmission lines: an effective approach based on the method of characteristics," *IEEE Trans. Advanced Packaging*, Vol.27, pp.45-56, February 2004.
7. A.Dounavis, R.Achar, M.Nakhla, ``A general class of passive macromodels for lossy multiconductor transmission lines ", *IEEE Trans. MTT*, Vol.49, 2001, 1686-1696.
8. A.Dounavis, N.Nakhla, R.Achar, M.Nakhla, ``Delay Extraction and Passive Macromodeling of Lossy Coupled Transmission Lines", in *Digest of Electr. Perf. Electronic Packaging*, Vol.12, Princeton, NJ, October 2003, pp.251-254.